Available online at www.sciencedirect.com
SCIENCE DIRECT
Journal of Power Sources 158 (2006) 326–332
JOURNAL OF POWER SOURCES
www.elsevier.com/locate/jpowsour

A novel technique for measuring current distributions in PEM fuel cells

Hong Sun [a,b], Guangsheng Zhang [a], Lie-Jin Guo [a,*], Hongtan Liu [a,c]

[a] *State Key Laboratory of Multiphase Flow in Power Engineering, Xi'an Jiaotong University, Xi'an, Shaanxi 710049, China*
[b] *Transportation and Mechanical Engineering Faculty, Shenyang Jianzhu University, Shenyang, Liaoning 110168, China*
[c] *Department of Mechanical and Aerospace Engineering, University of Miami, Coral Gables, FL 33124, USA*

Received 30 August 2005; accepted 12 September 2005
Available online 28 November 2005

Abstract

A novel and simple technique was developed to measure current distribution in PEM fuel cells with serpentine flow fields. In this technique, a specially designed measuring gasket was inserted between the flow field plate and the gas diffusion layer, and the current at each sub-area of the fuel cell was measured by each of the current collecting strips on the measuring gasket. The current distribution measurement gasket was independent of PEM fuel cells, and can be used in any fuel cell without the need of a special fuel cell or modification of any component of an existing fuel cell. More importantly, this technique can be easily used to measure current density distribution in any cell or every cell in a fuel cell stack. In addition, this technique is very inexpensive, with the only additional cost being that of the measuring gasket. In this work, this measurement gasket technique was used to study the influences of humidification temperatures, cell operating temperatures, reactant flow rates, and operating pressures on current distributions in a PEM fuel cell. Local membrane hydration, reactant depletion and possible cathode flooding can be deduced from the measurement results, and some potential improvements in fuel cell designs are suggested.

Keywords: PEM; Fuel cell; Current distribution; Measurement method

1. Introduction

Proton exchange membrane (PEM) fuel cells show tremendous promise as a future power system due to their high efficiency and low pollution. Many research efforts have been focused on improving PEM fuel cell performance [1–3]. Effective water management is required to achieve high performance, since water may accumulate in the cathode side due to water production and water transport by the electro-osmotic drag. The accumulated water may fill the pores of the gas diffusion layer and lead to significant loss in the PEM fuel cell performance. Thus, water transport as well as reactant transfer in PEM fuel cells has been one of the research focuses in the past 15 years [4–9].

In order to understand water transfer and current density variations in a fuel cell it is very important to measure local current distributions. Recently, much effort has been devoted to the development of techniques to measure local current densities in a fuel cell. Wieser et al. [10] developed a technique using a magnetic loop array embedded in the current collector plate to measure current distribution in PEM fuel cell. Stumper et al. [11] measured the current distribution using a partial membrane electrode assembly method, a sub-cell method, and a current mapping technique. Cleghorn et al. [12] demonstrated a method to measure current distribution in PEM fuel cells, using a printed circuit board technology to segment the current collector and flow field. Geiger et al. [13] described a new magnetic loop array with closed-loop Hall effect current sensors to measure current distribution in a PEM fuel cell. The segmented flow field approach [14] and its derivatives [15] are now popular techniques in measuring current distributions. Hakenjos et al. [16] developed a segmented anode flow field approach for current distribution measurement in PEM fuel cells.

All the techniques mentioned above require either specially designed fuel cells or modifications of collector plates and/or

* Corresponding author. Tel.: +86 29 8266 3895.
E-mail address: lj-guo@mail.xjtu.edu.cn (L.-J. Guo).

0378-7753/$ – see front matter © 2005 Elsevier B.V. All rights reserved.
doi:10.1016/j.jpowsour.2005.09.046

electrodes. Moreover, none of the existing method can be easily used in fuel cell stacks.

In this work, the simple and innovative current distribution measurement gasket technique was developed to measure current distribution in a PEM fuel cell with serpentine flow fields. The current distribution measurement gasket can be used in an existing fuel cell without modification of any of its components. More importantly, this technique can be easily used to measure the current density distribution in any or every cell in a fuel cell stack. This technique can also be easily adapted to other flow field designs. The measurement gasket is low-cost and simple.

2. Experimental

2.1. Current distribution measurement gasket

Fig. 1 shows the schematic diagram of the current distribution measurement gasket. The current distribution measurement gasket consists of a gasket with a pattern of the flow field used in the fuel cell. The substrate of the gasket is made of epoxy resin and glass cloth, the top surface is plated with copper and gold, and the measuring strips extend out of the cell for individual current measurement.

The measurement gasket used in this study is as shown in Fig. 2. In the case under study, 23 measuring strips are used. The overall dimension of the gasket is 11.6 cm long, 11.6 cm wide and 0.2 mm thick. The slots in the measurement gasket corresponding to flow channels in the flow field plate are 0.75 mm wide, and the strips corresponding to the shoulders in the flow field plate are 0.95 mm wide and 39.25 mm long. All strips are plated with copper and gold. The thickness of the copper is 30 μm and that of gold is 2 μm.

The PEM fuel cell used in the experiments is a single fuel cell with an active area of 16 cm^2. The flow field is single-channel serpentine, with 23 shoulders. The dimension of the flow field plate is 8.6 cm × 8.6 cm. The width of the flow channels is 0.75 mm and the depth is 1 mm. The width of the shoulders is 0.95 mm and the length is 39.25 mm. The total length of the serpentine flow channel is 1000 mm. The flow field in the anode is identical to that in the cathode and parallel flow (co-flow) is used in all the experiments reported in this study.

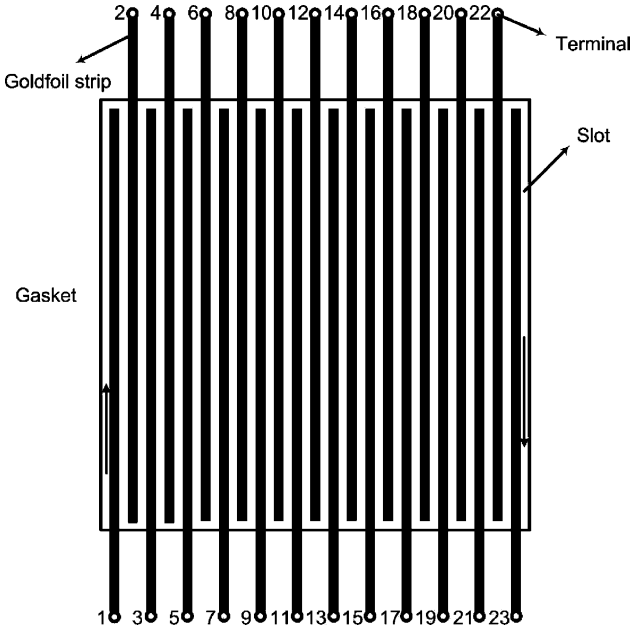

Fig. 1. Schematic diagram of current distribution measurement gasket.

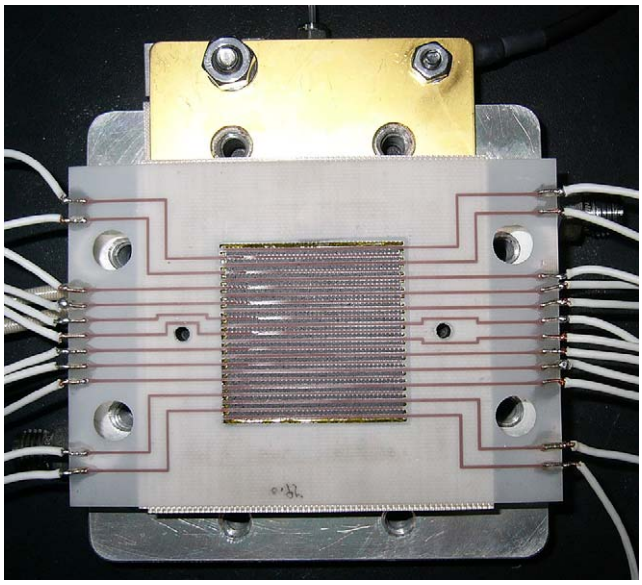

Fig. 2. A photograph of the current distribution measurement gasket.

2.2. Installation of the current distribution measurement gasket

The current measurement gasket is inserted between the flow field plate and the cathode gas diffusion layer, with the gold plated surface in direct contact with the gas diffusion layer, as shown in Fig. 3. Since the substrate is made of epoxy resin

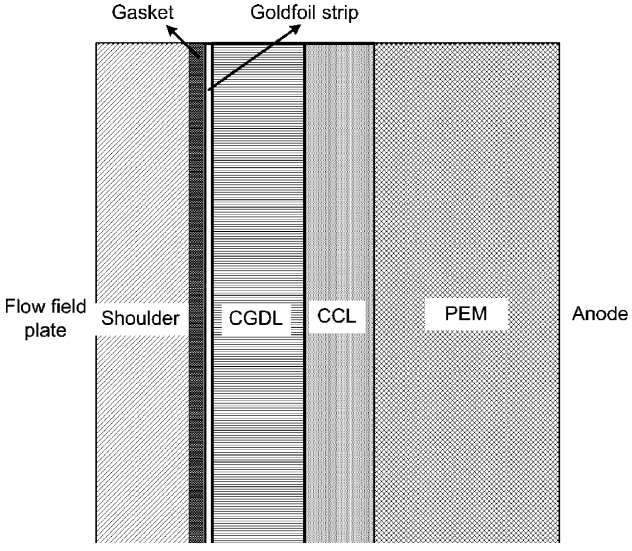

Fig. 3. Schematic of the position of the current measurement gasket in a PEM fuel cell.

and glass cloth, the measuring strips are insulated from each other and from the flow field; thus, the fuel cell is electrically divided into 23 local areas. The current from the 23 measuring strips are conducted out of the fuel cell laterally instead of to the shoulders of the flow field plate. Two alignment holes and careful cell assembly ensures good alignment of the measuring strips with the collector plate shoulders. In addition, uniform compression is important to minimize errors due to non-uniform contact resistance.

2.3. Current distribution measurement system

A flow diagram of the current distribution measurement experimental system is shown in Fig. 4. The fuel cell test system is controlled by a Labview™-based application software, which regulates reactant gas flow rates, fuel cell operating temperature, reactant humidification temperature, and operating pressure. Hydrogen and air/oxygen flow rates are controlled by two mass flow controllers, and their respective humidities are controlled by regulating the temperatures of the humidifiers. The operating pressures are regulated by adjusting the back-pressure regulators. A nitrogen purging system is incorporated into the experimental system to purge both the anode and cathode sides before and after experiments to ensure safety. The currents from the 23 measuring strips are measured by a 24-channel potentiostat with high-resolutions. The multi-channel potentiostat is controlled by a separate computer system using the MITS Pro™ software.

In this study, a single PEM fuel cell with an active area of 16 cm^2 was used. The membrane used was Nafion™ 112 with a thickness of 53 μm; the platinum catalyst loadings are 0.4 mg cm^{-2} on both sides. The gas diffusion layers (GDLs) were carbon fiber paper with 375 μm thickness. The flow field plates were made of graphite, and the flow fields are serpentine on both sides. The end plates were made of copper. Detailed information of the fuel cell used is listed in Table 1.

Table 1
Geometric parameters of the experimental fuel cell

Active area (cm^2)	16.0
Channel length (cm)	4.0
Channel width (cm)	0.075
Channel depth (cm)	0.095
Number of channels	24
Gas diffuser thickness (cm)	0.0375
Catalyst layer thickness (cm)	0.00129
Membrane thickness (cm)	0.0054

3. Results and discussion

The 23 measuring strips are numbered sequentially from the channel inlet to the outlet as shown in Fig. 1. Since the current density gradient across the fuel cell is small, symmetry can be assumed. Thus, each measuring strip measures the current from a local area covering one shoulder and two half-channels, except numbers 1 and 23, which cover an area of one shoulder plus one and one-half of a channel. Therefore, only the current data from strips 2 to 22 are used in the following presentations. Even though the current data from numbers 1 and 23 are not used in the final result analysis, these two strips must be put in place and connected to the same potentiostat to ensure the validity of the symmetry assumption for the two adjacent measuring strips.

3.1. Sample current density distributions

Fig. 5 shows local current density measurement results at three different cell voltages. Humidification temperatures on both the anode and cathode are set to the cell operating

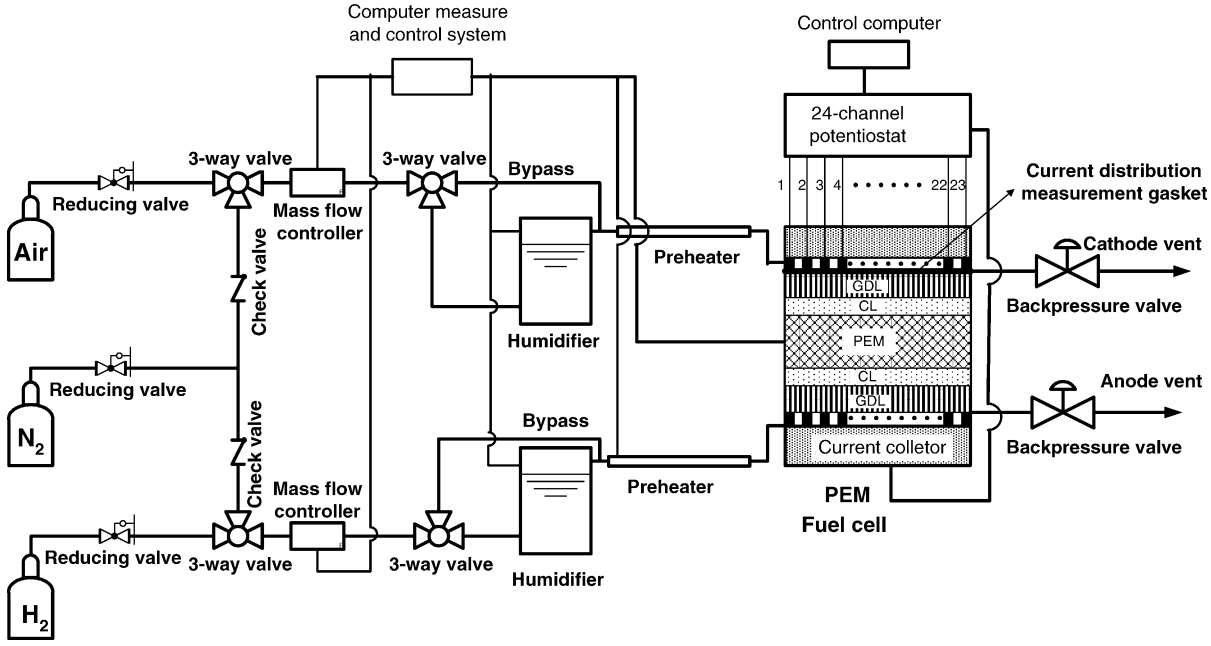

Fig. 4. Flow chart of the fuel cell current distribution measurement system.

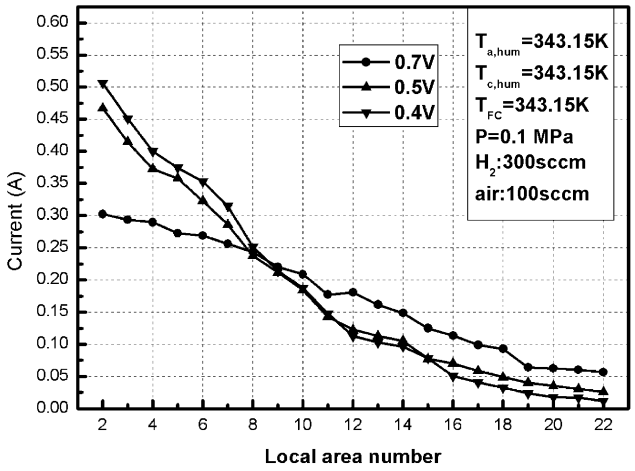

Fig. 5. Sample results of local current distribution at different cell voltages.

temperature to minimize the effects of variations in membrane conductivity and water flooding. It is easily seen that current density decreases along the flow direction. This is clearly caused by the decreased oxygen concentration along the flow direction, and possibly also by partial water flooding. At a lower cell voltage, the activation overpotential is higher and thus the current density is higher, as shown in Fig. 5 for a number of strips close to the inlet. Higher current density near the inlet causes a higher oxygen consumption rate and causes a lower oxygen concentration downstream. At a certain point, the effect of reduced oxygen concentration and possible flooding is greater than the effect of higher overpotential. Thus, local current density at a lower cell voltage becomes lower than those at a higher cell voltage. It is interesting to see from Fig. 5 that the current distribution for cell voltage at 0.5 V is very close to that for 0.4 V. This indicates that the cell is operating at or close to its local limiting current densities at every local area.

Fig. 6 shows the local polarization curves of current versus cell voltage for the case shown in Fig. 5. For ease of reading, only six representative local polarization curves are plotted instead of the entire 21. It is clearly seen from Fig. 6 that the performances of local areas from the entrance to the exit decrease due to the decrease of oxygen concentration, and possibly also the increase of flooding along the airflow direction. In this specific case, the airflow rate is 100 sccm. When the cell voltage is lower than 0.6 V, the current through local areas 16–22 is almost zero, indicating the depletion of oxygen. We can also see the typical "coma" shape of the polarization curves [16], showing the local limiting currents decrease due to the decrease of oxygen concentration in the channel at the local areas.

The results shown in Figs. 5 and 6 demonstrate the measurement gasket technique is suitable for measuring fuel cell local current density distributions. The measured current distributions are much smoother than most of the previous work [11,12,15,17–19], indicating that more uniform contact can be achieved using this technique.

3.2. Effects of air flow rates

Fig. 7 shows typical results of current distributions along the flow direction at different airflow rates. The general trends are the same for all flow rates with currents decreasing along the flow direction. At lower airflow rates, the decrease of current along the flow direction is steeper. This is caused by the greater percentage of decrease in oxygen concentration and possibly greater flooding since a lower velocity has a less effective water removal capability. For the 100 sccm flow rate case, local currents for the last areas are almost zero, which indicates the depletion of oxygen.

It is also seen that currents are higher at higher flow rates, and the differences are large, even at the inlet. This result indicates that at different flow rates, even if the local reactant concentrations are the same, the local current densities can still differ significantly. Thus, it can be deduced that the air velocity also plays a significant role in cell performance.

3.3. Effects of hydrogen flow rates

Fig. 8 shows the results of current density distribution along the flow direction at three different hydrogen flow rates. Since the airflow is at a very high rate of 900 sccm, the expected trend

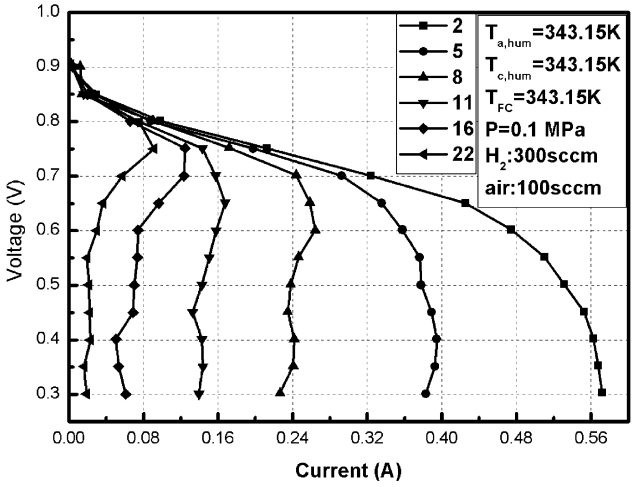

Fig. 6. Local polarizations of selected local areas.

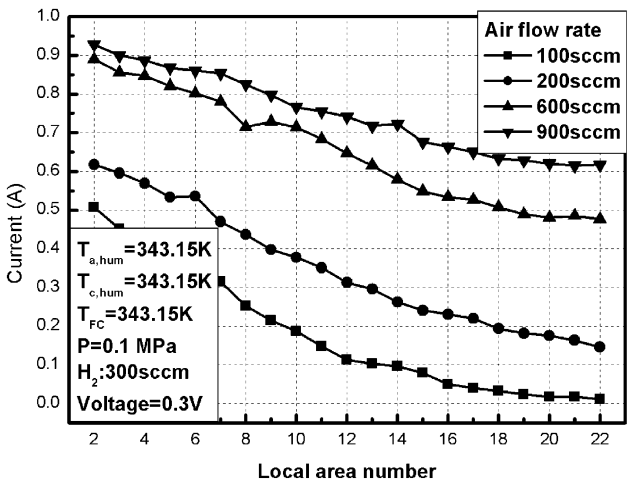

Fig. 7. Effect of air flow rates on current distributions.

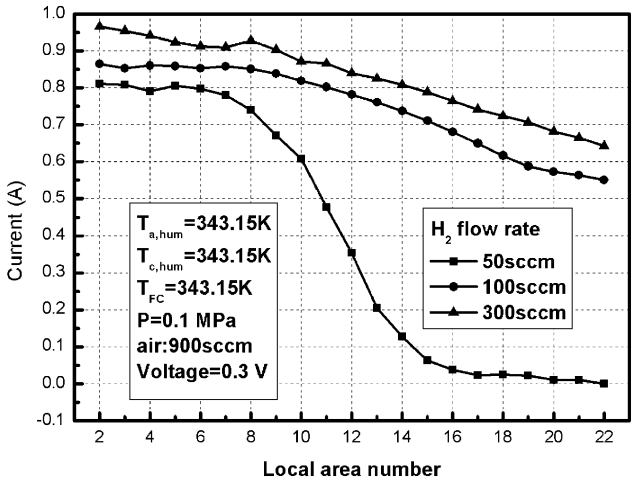

Fig. 8. Effects of hydrogen flow rate on local current distributions.

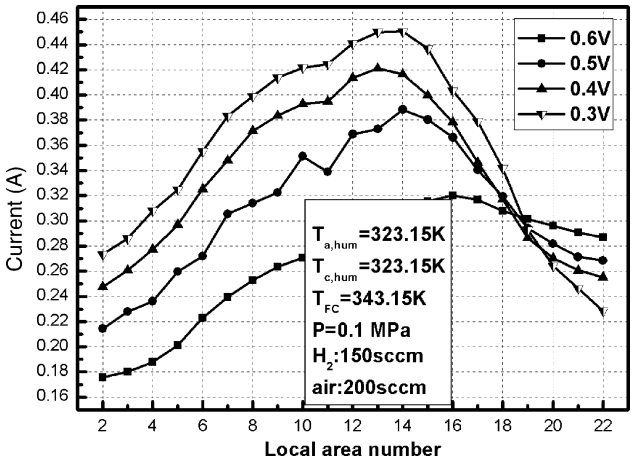

Fig. 9. Local current distributions at different cell voltages with insufficient humidification.

of current distribution is observed for both the flow rates of 300 and 100 sccm. It is clearly seen that the local currents for the case at 100 sccm are always lower than those at 300 sccm. Since all the other operating conditions are the same, the difference in local currents, ranging from 0.05 to 0.1 A, can be attributed to the effect of anode flow rate. This result shows that effects of the anode side are not negligible, indicating that the widely held assumption [20] needs to be re-evaluated. For a hydrogen flow rate at 50 sccm, the currents at local areas 8–14 decrease sharply, and tend to zero from areas 16 to 22, indicating the depletion of hydrogen in the later part of the cell. This experimental result shows that either the pressure-drop along the channel is significant, or the net water transfer coefficient λ (for its definition, see [8]) is less than 0.5, i.e., less than half a water molecule is transferred per hydrogen molecule consumed.

3.4. Effects of humidification temperatures

It is well known that reactant humidity plays a critical role in the performance of PEM fuel cells. The humidity of the reactant gases is generally regulated by controlling the humidification temperature. Fig. 9 shows a set of current distributions at different cell voltages. Note that the humidification temperatures for both the anode and cathode are 323.15 or 20 K degrees lower than the cell operating temperature of 343.15 K. For each case, the local current starts very low at the inlet, increases along the channel, reaches a maximum, and then decreases further down the stream. Since the humidification temperatures are lower than the cell temperature, the membrane is relatively dry close to the inlet, leading to a lower current density. Along the channel direction, more and more water is produced and the membrane becomes better and better hydrated, increasing the current. Further down the stream, even though the membrane may be well-hydrated, the effect of reduced reactant concentration becomes dominant and causes the current to decrease. In short, this set of experimental results shows the opposite effects of membrane hydration and reactant concentration reduction at play.

It can also be seen from Fig. 9 that the higher the current is in the upstream, the sharper the current drop is in the downstream. The sharper drop in current is caused by the lower local reactant concentrations. When the current density is higher in the upstream, more reactants are consumed, resulting in a lower reactant concentration in the downstream, causing a lower current.

To facilitate understanding, seven selected local polarization curves from the same experiment shown in Fig. 9 are presented in Fig. 10. At low currents, the effect of reactant concentrations is not significant and the effect of membrane resistance is dominant. Along the gas channel, water produced by the electrochemical reaction causes the membrane to be better hydrated, and the resistance decreases, increasing the local current along the channel. At high current densities, the areas close to the end of the channel are deprived of reactants and their performances are lower than their upstream neighbors.

It can be seen from Figs. 5–8 that when there is enough humidification, the local current decreases along the channel direction, and from Figs. 9 and 10 that the local current first increases, then decreases after reaching a maximum. To cover all the

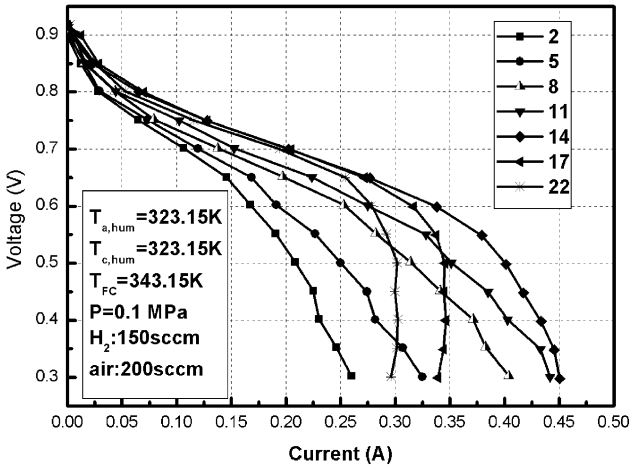

Fig. 10. Selected local polarization curves under insufficient humidification.

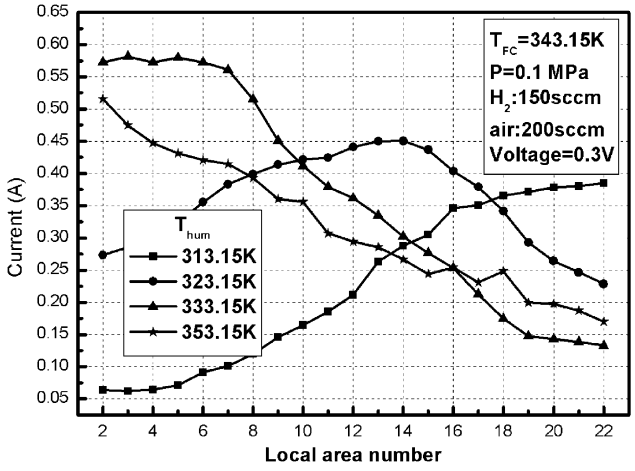

Fig. 11. Local current distributions at various humidification temperatures.

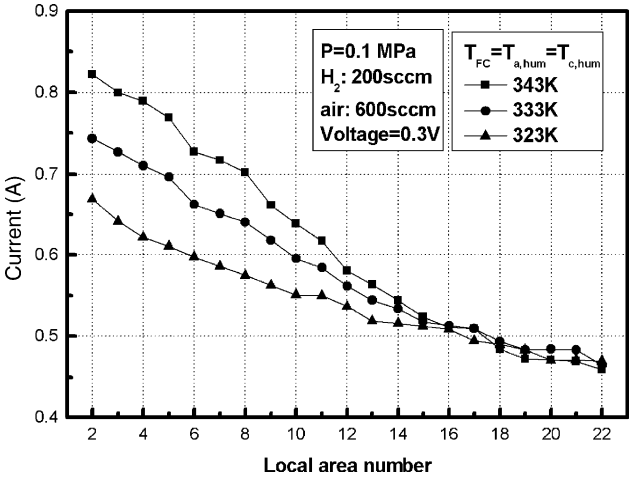

Fig. 12. Effects of fuel cell operating temperature on fuel cell local current distributions.

scenarios, current distributions at four different humidification temperatures are presented in Fig. 11. Note that for all cases, the humidification temperature at the anode and cathode are the same.

When the humidification temperature is at 313.15 K, 30 K below the cell temperature, the local currents close to the inlet are very low, indicating a dry membrane. Along the channel, local currents increase due to water generation and accumulation. Local currents monotonically increase until the end of the channel, never peaking. This indicates that under such dry conditions, the membrane never full hydrates, even as it reaches the end of the channel. It is also interesting to note that the curve is concave in the early part and convex in the later part. In the early part, local currents are low and the effect of reactant concentration is negligible. The dominant effect is the membrane hydration, which increases at a rate directly related to water production rate, which is directly related to local current density. Therefore, the slope of the curve increases as the local current increases. Later on, the convexity of the curve is caused by the coupled effect of membrane hydration and reactant concentration reduction.

When the humidification temperature is at 323.15 K, 20 K below the fuel cell operating temperature, the current distribution curve does have a peak, as explained earlier. When the humidification temperature is at 333.15 K, 10 K below the fuel cell operating temperature, the current in the first a few areas is almost constant, indicating that the effect of increasing membrane hydration is canceled by the effect of decreasing reactant concentration. After the membrane is fully hydrated, the effect of decreasing reactant concentration plays a dominant role and the current decreases along the channel. When the humidification temperature is at 353.15 K, 10 K above the fuel cell operating temperature, the local current steadily decreases along the channel.

3.5. Effect of operating temperatures

Fig. 12 shows the results of current distributions under three different operating temperatures. In order to minimize the effect of gas stream humidification, the humidification temperatures for both the anode and cathode are set to the cell operating temperature. As expected, the cell performance increases with cell temperatures, and the local current decreases along the channel. This can be seen in Fig. 12.

3.6. Effects of operating pressures

Fig. 13 shows the results of current distributions at three different operating pressures. Again the expected trends are observed. The cell performance increases with operating pressure due to increased electrochemical activities and higher open-circuit voltages. It can also be seen that at a higher pressure, the local current is higher close to the inlet, but lower in the later part of the channel. This result reveals that the advantage of higher operating pressures can be considerably reduced due to poor performance in the downstream of the channels. Therefore, to fully take advantage of higher operating pressures, shorter gas channels should be used.

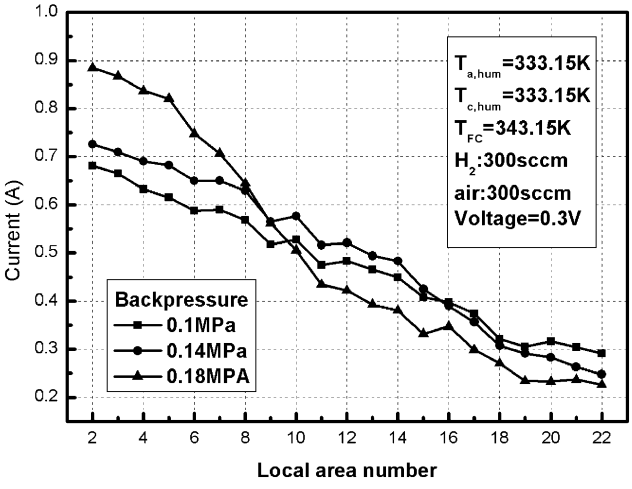

Fig. 13. Effects of operating pressures on local current distributions.

4. Conclusions

A novel and simple technique is developed for the measurement of local current distributions in PEM fuel cells with serpentine flow fields using a measurement gasket. To measure current distributions, there is no need to change the electrode structures and/or flow field plates; rather, the measurement gasket only needs to be inserted between the flow field plate and the gas diffusion layer. This technique is very inexpensive as the only additional cost is the measuring gasket. As local currents are conducted out of the cell laterally, this technique can also be easily used in a fuel cell stack to measure current distributions in any single cell, any number of cells, or even all the cells. This innovative technique is used to measure local current distributions of a PEM fuel cell at various operating conditions; the following conclusions can be drawn based on the measurement results.

- Experimental results show that this technique is suitable for measuring fuel cell local current distributions, and the measured results are better than many of the more complicated techniques.
- Air flow rates have a significant effect on cell performance; the local current distributions have a similar pattern for all air flow rates: decreasing along the channel. At very low air flow rates, the later parts of the cell are starved of oxygen and local currents approach zero.
- Hydrogen flow rates also have an effect on cell performances, though not as significant as that of air flow rates. At very low hydrogen flow rates, later parts of the cell are starved of hydrogen and the current tends to zero, revealing that either the pressure drop along the channel is significant or the net water transfer coefficient is less than 0.5.
- Gas humidification is critical in fuel cell current distributions. At very low humidification, the cell performance is poor and the local current increases monotonically along the channel; at medium humidification, the local currents first increase along the channel, then decrease; at high humidification, the local current decrease monotonically along the channel.
- Fuel cell performance increases with increased operating temperature as expected; this is mainly achieved in the upstream of the cell.
- Fuel cell performance increases with increased operating pressure as expected; this result indicates that higher operating pressures would benefit from shorter gas channels.

Acknowledgment

Financial support from the National Natural Science Foundation of China for Distinguished Young Overseas Chinese Scholar under contract 50228606 and the National Basic Research Program of China under contract 2003CB214500 is gratefully appreciated.

References

[1] L.R. Jordan, A.K. Shukla, T. Behrsing, N.R. Avery, B.C. Muddle, M. Forsyth, Diffusion layer parameters influencing optimal fuel cell performance, J. Power Sources 86 (2000) 250–254.
[2] P. Sridhar, R. Perumal, N. Rajalakshmi, M. Raja, K.S. Dhathathreyan, Humidification studies on polymer electrolyte membrane fuel cell, J. Power Sources 101 (2001) 72–78.
[3] L. Wang, A. Husar, T. Zhou, H. Liu, A parametric study of PEM fuel cell performances, Int. J. Hydrogen Energy 28 (2003) 1263–1272.
[4] V. Gurau, H. Liu, S. Kakac, Two-dimensional model for proton exchange membrane fuel cells, AIChE J. 44 (1998) 2410–2422.
[5] T. Zhou, H. Liu, A general three-dimensional mode for proton exchange membrane fuel cells, Int. J. Trans. Phenomena 3 (2001) 177–198.
[6] D. Natarajan, T.V. Nguyen, A two-dimensional, two-phase, multicomponent, transient model for the cathode of a proton exchange membrane fuel cell using conventional gas distributors, J. Electrochem. Soc. 148 (12) (2001) A1324–A1335.
[7] Z.H. Wang, C.Y. Wang, K.S. Chen, Two-phase flow and transport in the air cathode of proton exchange membrane fuel cells, J. Power Sources 94 (2001) 40–50.
[8] L. You, H. Liu, A two-phase flow and transport model for the cathode of PEM fuel cells, Int. J. Heat Mass Transfer 45 (2002) 2277–2287.
[9] H. Sun, H. Liu, L.J. Guo, PEM fuel cell performance and its two-phase mass transport, J. Power Sources 143 (2005) 125–135.
[10] Ch. Wieser, A. Helmbold, E. Gulzow, A new technique for two-dimensional current distribution measurements in electrochemical cells, J. Appl. Electrochem. 30 (2000) 803–807.
[11] J. Stumper, S.A. Campbell, D.P. Wilkinson, In-situ method for the determination of current distribution in PEM fuel cells, Electrochim. Acta 43 (24) (1998) 3773–3783.
[12] S.J. Cleghorn, C.R. Derouin, M.S. Wilson, S. Gotterfeld, A printed circuit board approach to measuring current distribution in a fuel cell, J. Appl. Electrochem. 28 (1998) 663–672.
[13] A.B. Geiger, R. Eckl, a. Wokaun, G.G. Scherer, J. Electrochem. Soc. 151 (3) (2004) A394–A398.
[14] M. Noponen, T. Mennola, M. Mikkola, T. Hottinen, P. Lund, Measurement of current distribution in a free-breathing PEMFC, J. Power Sources 106 (2002) 304–312.
[15] M.M. Mench, C.Y. Wang, M. Ishikawa, In situ current distribution measurements in polymer electrolyte fuel cells, J. Electrochem. Soc. 150 (8) (2003) A1052–A1059.
[16] A. Hakenjos, H. Muenter, U. Wittstadt, C. Hebling, A PEM fuel cell for combined measurement of current and temperature distribution, and flow field flooding, J. Power Sources 131 (2004) 213–216.
[17] Z. Liu, Z. Mao, B. Wu, L. Wang, V.M. Schmidt, Current density distribution in PEFC, J. Power Sources 141 (2005) 205–210.
[18] N. Rajalakshmi, M. Raja, K.S. Dhathathreyan, Evaluation of current distribution in a proton exchange membrane fuel cell by segmented cell approach, J. Power Sources 112 (2002) 331–336.
[19] D. Brett, S. Atkins, N. Brandon, V. Vesovic, N. Vasileiadis, A. Kucernak, Measurement of the current distribution along a single flow channel of a solid polymer fuel cell, Electrochem. Commun. 3 (2001) 628–632.
[20] P. Berg, K. Promislow, J. Pierre, J. Stumper, Water management in PEM fuel cells, J. Electrochem. Soc. 151 (3) (2004) A341–A353.